Beacon-assisted Underwater Localization by L1-norm Space-Time Tensor Subspaces

Konstantinos Tountas,[†] George Sklivanitis, and Dimitris A. Pados

I-SENSE and Dept. of Computer and Electrical Engineering & Computer Science, Florida Atlantic University
E-mail: {ktountas2017, gsklivanitis, dpados}@fau.edu

***Abstract*—We consider the problem of robust self-localization of underwater robots with no GPS assistance and no availability of global clock synchronization. In particular, we consider self-localization of autonomous underwater vehicles that are equipped with a triangular hydrophone acoustic array and leverage time-domain coded beacons from two single-hydrophone acoustic nodes that are placed at known locations. Collected data snapshots over time at the hydrophone array are organized in a tensor data structure. Highly robust iteratively refined L_1-norm space-time tensor subspaces that are calculated at the underwater acoustic array receiver allow accurate estimation of the azimuth and elevation angles-of-arrival and codes of the two beacons. The relative position of the vehicle with respect to the two beacons can then be estimated via triangulation. Simulation studies over statistically modeled underwater acoustic communication channels verify that the proposed beacon-assisted localization technique offers superior positioning accuracy than state-of-the-art methods that rely on L_2-norm based MUltiple-SIgnal-Classification (MUSIC) estimation of the angles-of-arrival and codes of the beacons.**

I. Introduction

Autonomous underwater vehicles (AUVs) have attracted considerable attention for both military, scientific and industrial applications including deep-sea oceanographic exploration [1], scientific sampling [2], subsea search-and-rescue [3], reconnaissance operations [4], pollution monitoring and aqua-farming [5]. An important challenge in the deployment of AUVs is self-localization of the underwater vehicle that cannot access GPS satellite links. Self-localization of AUVs relatively to known location GPS-assisted surface buoys or other vehicles in swarm deployment can help the vehicle navigate in the unknown deep-sea environment, reliably communicate and network with other vehicles and stamp collected sensor data with a spatial reference.

GPS-free localization schemes proposed for terrestrial radio networks involve intensive message exchanges, and therefore are not suitable for the low-bandwidth, high-latency underwater acoustic (UW-A) channel. Existing state-of-the-art approaches for undersea localization and tracking of AUVs either consider expensive inertial sensors [6], geophysical-based [7], or acoustic communication techniques [8]. Acoustic-based localization techniques rely on angle or distance measurements between wirelessly communicating nodes that are collected by received-signal-strength (RSS), time-of-arrival (ToA), time-of-flight (ToF), time-difference-of-arrival (TDoA), and angle-of-arrival (AoA) techniques. For example, long baseline (LBL) and Ultra-Short Base-Line (USBL) involve acoustic transponders that are used as reference nodes for underwater localization and navigation. Both LBL and USBL employ TDoA techniques between time-synchronized transponders [9]. Localization costs incurred by the complex deployment and clock synchronization requirements of distributed transponders are addressed by the range-only single-beacon (ROSB) method in [10], [11]. The ROSB method is based on tracking underwater targets/assets by controlling the maneuvers of an underwater vehicle. The vehicle periodically performs slant range measurements using the ToF of messages exchanged with underwater targets/assets [12]. The above localization techniques offer good accuracy under nominal operation conditions. However, their performance significantly degrades in the presence of outlier measurements due to intermittent environmental disturbances, and hardware and/or channel impairments (such as channel path variations, impulsive noise sources, and faulty measurements).

Sonar-based localization techniques utilize seabed images generated from measuring the intensity of sonar reflected signals. Features extracted from these images are then used for data association in simultaneous-localization-and-mapping (SLAM) methods [13]. Most SLAM-based techniques rely on filtering algorithms such as extended Kalman filtering (EKF) and particle filtering (PF) [14] to address linearization errors and reduce computational cost. In [15] the smooth variable structure filter method is introduced to solve the SLAM problem. The proposed method is proven to be robust to modeling errors and uncertainties by utilizing existing subspace information and a smoothing layer to keep the location estimates bounded within a region of the true state trajectory.

Direction-of-arrival (DoA)-guided localization methods typically utilize subspace-based parameter estimation techniques based on L_2-norm or L_1-norm principal-component analysis (PCA) [16]. In [17] a particle filter is used for DoA estimation of an acoustic source. Existing approaches for subspace-based parameter estimation [16], [18] rely on organization of the collected data snapshots at the receiver

This work was supported by the National Science Foundation under Grant CNS-1753406. The work of D. A. Pados was also supported by the Schmidt Family Foundation.

[‡]Principal author: Konstantinos Tountas, Research Assistant, Department of Computer and Electrical Engineering & Computer Science, Florida Atlantic University, FL 33431, USA.

978-0-578-57618-3 ©2019 MTS

array in matrices by means of the stacking operation. Matrix representation clearly does not account for the grid structure that is inherent in the wireless channel data recordings. A more natural approach to store and manipulate multidimensional data is given by tensors. In this paper, we show that the tensor representation allows us to fully exploit the structure of underwater acoustic space-time coded data as these arrive at the input of an acoustic array. More specifically, we consider the deployment of an autonomous underwater vehicle that is equipped with an equilateral triangular hydrophone acoustic array. The AUV can robustly self-localize in 3D by accurately estimating the codes and azimuth and elevation angles-of-arrival of the transmitted beacons from two reference nodes. The beacons are single-hydrophone acoustic nodes that are deployed in known locations and transmit time-domain coded signals in a spread-spectrum fashion. Orthogonal codes of length L enable simultaneous beacon transmissions in frequency and time. We consider that all transmitted beacons propagate over UW-A multipath fading channels. The received beacons at the input of the hydrophone array are then organized in a tensor structure. We show, for the first time, that underwater acoustic DoA estimation through L_1 norm space-time tensor subspaces significantly outperforms both L_2-norm PCA-based tensor and matrix processing methods, thus offering superior underwater positioning accuracy. Simulation studies are conducted over multipath and Doppler spread channels that are generated by an UW-A channel simulator [19].

II. System Model

We consider underwater acoustic transmissions from K asynchronous single-hydrophone UW-A beacons over single-input multiple-output (SIMO) frequency-selective fading channels with M resolvable paths as depicted in Fig. 1. The transmitted signal of the k-th acoustic beacon is written as

$$x_k(t) = \sqrt{E_k} \sum_n b_k[n] s_k(t - nT) e^{j(2\pi f_c t + \phi_k)} \tag{1}$$

where ϕ_k is the carrier phase, f_c is the carrier center acoustic frequency and the n-th symbol for the k-th user $b_k[n]$ is drawn from a complex constellation $\mathcal{C}$ of energy $E_k > 0$, and modulated by an all-spectrum digital waveform $s_k(t)$ that is given by

$$s_k(t) = \sum_{l=0}^{L-1} \mathbf{d}_k[l] g_{T_c}(t - lT_c) \tag{2}$$

where $\mathbf{d}_k \in \left\{ \pm \frac{1}{\sqrt{L}} \right\}^L$ is a binary code of length L, and $g_{T_c}(\cdot)$ is a square-root raised cosine (SRRC) pulse with roll-off factor α and duration T_c, so that $T = LT_c$. The bandwidth of the k-th transmitted signal is $B = (1+\alpha)/T_c$.

We assume that transmitted signals propagate over independent time-varying frequency-selective UW-A channels with M resolvable paths, with $a_{k,m}(t)$ and $\tau_{k,m}(t)$ denoting the m-th path's time-varying amplitude coefficient and path delay for the k-th user, respectively. For mathematical tractability, we assume that $\tau_{k,m}(t)$ can be approximated by a first-order polynomial $\tau_{k,m}(t) = \tau_{k,m} - \beta_{k,m} t$, where $\beta_{k,m} = u_{k,m}/c$, $u_{k,m}$ is the radial velocity of the m-th path and c is the speed of sound in water. After multipath fading channel "processing", the received signal at the input of an equilateral triangular array with 3 elements is given by

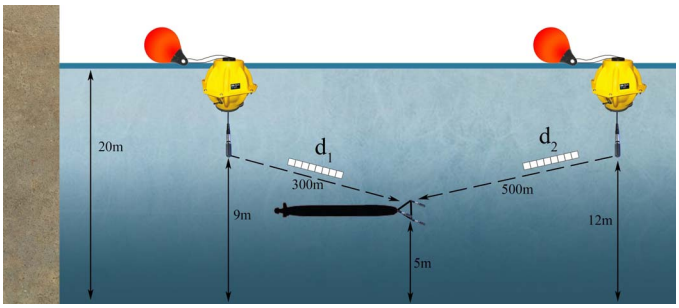

Fig. 1. System setup of $K = 2$ single-hydrophone underwater acoustic beacons and a triangular hydrophone acoustic array receiver.

$$\mathbf{y}(t) = \sum_{k=0}^{K-1} \sum_{m=0}^{M-1} \mathbf{a}(\phi_k, \theta_k)\, a_m(t) x_k(t(1+\beta_m) - \tau_m) + \mathbf{n}(t) \tag{3}$$

where $\mathbf{a}(\phi_k, \theta_k) \in \mathbb{C}^3$ is the hydrophone array response vector for the k-th beacon defined as

$$\mathbf{a}(\phi, \theta) = \exp\left\{ j2\pi \frac{1}{\lambda_c} \mathbf{P}^T \mathbf{k}(\phi, \theta) \right\} \in \mathbb{C}^{3\times 1} \tag{4}$$

where λ_c is the carrier wavelength, the matrix $\mathbf{P}$ contains the hydrophone array element values

$$\mathbf{P} = \begin{bmatrix} x_1 & x_2 & \dots & x_D \\ y_1 & y_2 & \dots & y_D \\ z_1 & z_2 & \dots & z_D \end{bmatrix} \in \mathbb{R}^{3\times 3} \tag{5}$$

and the vector $\mathbf{k}(\phi, \theta)$ represents the projection of the received signal's steering vector on the hydrophone array coordinate system defined as

$$\mathbf{k}(\phi, \theta) = \begin{bmatrix} \cos(\theta)\sin(\phi) \\ \cos(\theta)\cos(\phi) \\ \sin(\theta) \end{bmatrix} \in \mathbb{R}^{3\times 1}. \tag{6}$$

The carrier demodulated and pulse-matched filtered received signal vector after sampling over the symbol duration and buffering $L_M = L + M - 1$ samples, the n-th received space-code data snapshot is written as

$$\mathbf{Y}_n = \sum_{k=1}^{K} \sqrt{E_k} b_k[n]\, \mathbf{a}(\phi_k, \theta_k) \left(\mathbf{H}_k \mathbf{d}_k\right)^T + \mathbf{J}_n + \mathbf{N}_n \in \mathbb{C}^{3\times L_M} \tag{7}$$

where $\mathbf{H}_k \in \mathbb{C}^{L_M \times L}$ is the multipath channel matrix for the k-th beacon, which is assumed to be invariant over channel coherence time T_{coh}. We assume the same fading and multipath fading across all the array elements for each beacon. Colored interference by $\mathbf{J}[n] \in \mathbb{C}^{3\times L_M}$ models colored interference at the input of the hydrophone array, and $[\mathbf{N}[n]]_{i,j}$ is an additive noise component.

Ambient noise in the underwater acoustic channel is frequency-dependent and produced by sources such as turbulence, wave action, ship traffic, and thermal noise from random

motion of water molecules [20]. The power spectral density of ambient UW-A noise can be approximated as[1]

$$N_{\text{AVG}}(f) = 50 - 18\log(f) \text{ dB re } \mu\text{Pa/Hz} \quad (8)$$

for frequency f in kHz [21].

By defining the power-scaled signature matrix $\mathbf{S} = [\mathbf{s}_1, \ldots, \mathbf{s}_K] \in \mathbb{R}^{L_M \times K}$, where $\mathbf{s}_k = \sqrt{P_k}\mathbf{H}_k\mathbf{d}_k$, the rank-3 steering matrix $\mathbf{A} = [\mathbf{a}(\phi_1, \theta_1), \ldots, \mathbf{a}(\phi_K, \theta_K)] \in \mathbb{C}^{3\times K}$, and a diagonal matrix $\mathbf{B}[n] = diag([b_1[n], b_2[n], \ldots, b_K[n]])$, the n-th received data snapshot matrix in (7) can be expressed in the following matrix form

$$\mathbf{Y}_n = \mathbf{A}\mathbf{B}_n\mathbf{S}^T + \mathbf{J}_n + \mathbf{N}_n \in \mathbb{C}^{3\times L_M}, \quad n = 1, 2, \ldots, N. \quad (9)$$

We observe that the received matrices can be viewed as slices of an $3 \times L_M \times N$ three-way tensor $\mathcal{Y} \in \mathbb{C}^{3\times L_M \times N}$. Our goal is to utilize the tensor structure of our data in order to accurately estimate the angles of arrival, as well as identify the waveforms the beacons are using.

III. Direction-of-Arrival Estimation through L_1-norm Space-time Tensor Subspaces

A. Preliminaries

We begin our algorithmic developments by defining the real-valued representation $\overline{\mathbf{A}} \in \mathbb{R}^{2m\times 2n}$ of any complex-valued matrix $\mathbf{A} \in \mathbb{C}^{m\times n}$ by concatenating real and imaginary parts as follows

$$\overline{\mathbf{A}} = \begin{bmatrix} \text{Re}\{\mathbf{A}\}, & -\text{Im}\{\mathbf{A}\} \\ \text{Im}\{\mathbf{A}\}, & \text{Re}\{\mathbf{A}\} \end{bmatrix} \in \mathbb{R}^{2m\times 2n} \quad (10)$$

where $\text{Re}\{\cdot\}$ and $\text{Im}\{\cdot\}$ return the real and imaginary part of each matrix element, respectively. The transition from $\mathbf{A} \in \mathbb{C}^{m\times n}$ to $\overline{\mathbf{A}} \in \mathbb{R}^{2m\times 2n}$ is based on what is commonly referred to as complex-number *realification* in representation theory. Realification allows for any complex system of equations to be converted and solved through a real system.

B. DoA Estimation and Beacon Identification

By (10), we define the n-th "*realified*" snapshot $\overline{\mathbf{Y}}_n$ as

$$\overline{\mathbf{Y}}_n = \overline{\mathbf{A}}\,\overline{\mathbf{B}}_n\,\overline{\mathbf{S}}^T + \overline{\mathbf{N}}_n \in \mathbb{R}^{6\times 2L_M}, \quad n = 1, 2, \ldots, N. \quad (11)$$

With the realification operation, we convert our complex tensor $\mathcal{Y} \in \mathbb{C}^{3\times L_M \times N}$ to a real-valued tensor $\overline{\mathcal{Y}} \in \mathbb{R}^{6\times 2L_M \times N}$. From (11), we notice that the angle components of interest lie in the $R_1 \geq 2K$ dimensional space $\mathcal{S}_A = \text{span}\left(\overline{\mathbf{A}}\right)$, while the code components of interest lie in the $2K$ dimensional space $\mathcal{S}_D = \text{span}\left(\overline{\mathbf{S}}\right)$. The following propositions highlight the utility of $\mathcal{S}_A$ and $\mathcal{S}_D$ for estimating the target directions of arrival (DoA's) and code sequences in $\mathcal{A}$ and $\mathcal{D}$, respectively.

Proposition 1. *For any pair* $(\phi, \theta) \in \left(-\frac{\pi}{2}, \frac{\pi}{2}\right]$, $\text{span}\left(\overline{\mathbf{a}}(\phi, \theta)\right) \subseteq \mathcal{S}_A$ *if and only if* $(\phi, \theta) \in \mathcal{A}$. *Set equality holds only if* $K = 1$.

[1]The term re μPa denotes with reference to the intensity of a plane wave with RMS pressure of 1 μPa. Unless otherwise specified, this reference is considered to be at a distance of 1 m from the sound source.

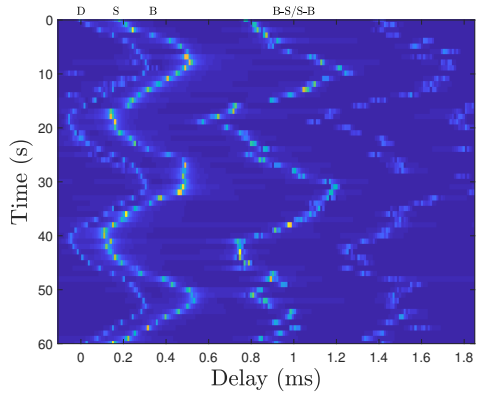

Fig. 2. Relative magnitude and time delay of channel paths over time for the link between the first beacon node (300 m), and the hydrophone array. Labels denote the direct (D) path, surface reflection (S), bottom reflection (B), and the bottom-surface (B-S) and surface-bottom (S-B) reflections which should arrive approximately simultaneously.

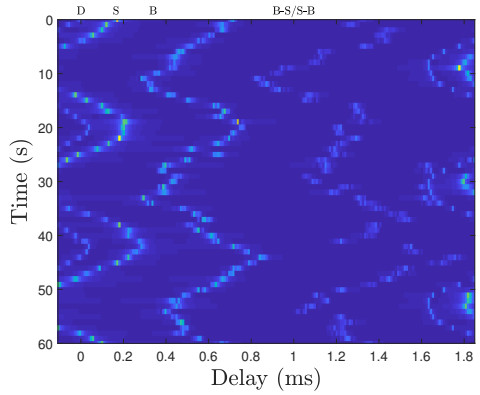

Fig. 3. Relative magnitude and time delay of channel paths over time for the link between the second beacon node (500 m), and the hydrophone array.

By proposition 1, we can accurately decide whether some pair $(\phi, \theta) \in \left(-\frac{\pi}{2}, \frac{\pi}{2}\right]$ is a target DoA or not by means of any orthonormal basis $\mathbf{Q}_1 \in \mathbb{R}^{6\times 2K}$ that spans $\mathcal{S}_A$ as

$$\left(\mathbf{I}_6 - \mathbf{Q}_1\mathbf{Q}_1^T\right)\overline{\mathbf{a}}(\phi, \theta) = \mathbf{0}_{6\times 2} \Leftrightarrow (\phi, \theta) \in \mathcal{A}. \quad (12)$$

Thus, in view of proposition 1, and in accordance to common practice, target DoAs in $\mathcal{A}$ can be approximated by the K highest peaks of the MUSIC-like pseudo-spectrum defined as

$$P_A(\phi, \theta) = \left\|\left(\mathbf{I}_6 - \mathbf{Q}_1\mathbf{Q}_1^T\right)\overline{\mathbf{a}}(\phi, \theta)\right\|^{-2} \quad (13)$$

The same holds for the waveform estimation problem, as stated in the following proposition.

Proposition 2. *For any* $\mathbf{d} \in \left\{\pm\frac{1}{\sqrt{L}}\right\}^L$, $\text{span}\left(\overline{\mathbf{d}}\right) \subseteq \mathcal{S}_D$ *if and only if* $\mathbf{d} \in \mathcal{D}$. *Set equality holds only if* $K = 1$.

By proposition 2, the target sequences can be estimated by any $R_2 \geq 6$ dimensional orthonormal basis $\mathbf{Q}_2 \in \mathbb{R}^{2L_M\times 2K}$ that spans $\mathcal{S}_D$ as

$$\left(\mathbf{I}_6 - \mathbf{Q}_2\mathbf{Q}_2^T\right)\overline{\mathbf{d}} = \mathbf{0}_{6\times 2} \Leftrightarrow \overline{\mathbf{d}} \in \mathcal{D}. \quad (14)$$

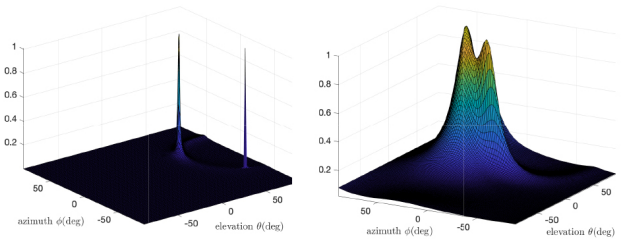

Fig. 4. Azimuth and elevation pseudo-spectra for L_1-norm [26] (Left) and L_2-norm tensor decompositions [22] (Right) before the estimation of the the beacon nodes' codes.

And the corresponding pseudo-spectrum is

$$P_D\left(\overline{\mathbf{d}}\right) = \left\|\left(\mathbf{I}_{2L_M} - \mathbf{Q}_2\mathbf{Q}_2^T\right)\overline{\mathbf{d}}\right\|^{-2}. \tag{15}$$

Peaks in the two pseudo-spectra in (13) and (15) identify DoAs and waveform sequences without uniquely associating angles and sequences. In order to have this correspondence, we create all possible DoA pairs and waveform sequence candidates as

$$\mathbf{z}\left(\phi,\theta,\mathbf{d}\right) = \mathbf{a}\left(\phi,\theta\right)\otimes\mathbf{d} \in \mathbb{C}^{3L_M\times 1}. \tag{16}$$

Then, we calculate the K principle components, $\mathbf{Q}_{sc}$, of the space-code matrix $\mathbf{Y}_{sc} = \left[\mathrm{vec}\left(\mathbf{Y}_1\right),\ldots,\mathrm{vec}\left(\mathbf{Y}_N\right)\right]$ by means of SVD. We utilize the following pseudo-spectrum to find the peaks corresponding to the exact DoAs and waveform sequence associations

$$P_{SC}\left(\mathbf{z}\right) = \left\|\left(\mathbf{I}_{3L_M} - \mathbf{Q}_{sc}\mathbf{Q}_{sc}^H\right)\mathbf{z}\right\|^{-2}. \tag{17}$$

C. L_2-norm Tensor Subspaces

Following the TUCKER tensor model, the L_2-norm tensor subspace estimation problem for a 3-dimensional tensor $\mathcal{X} \in \mathbb{R}^{D\times L\times N}$ can be written as

$$\left(\widehat{\mathbf{Q}_1},\widehat{\mathbf{Q}_2},\widehat{\mathbf{Q}_3}\right) = \underset{\substack{\mathbf{U}\in\mathbb{R}^{D\times R_1},\mathbf{Q}_1^T\mathbf{Q}_1=\mathbf{I}_{R_1},\\ \mathbf{Q}_2\in\mathbb{R}^{L\times R_2},\mathbf{Q}_2^T\mathbf{Q}_2=\mathbf{I}_{R_2},\\ \mathbf{Q}_3\in\mathbb{R}^{N\times R_3},\mathbf{Q}_3^T\mathbf{Q}_3=\mathbf{I}_{R_3}}}{\mathrm{argmax}} \left\|\mathbf{Q}_1^T\mathbf{X}_{(1)}\left(\mathbf{Q}_2\otimes\mathbf{Q}_3\right)\right\|_F^2 \tag{18}$$

where $\|\cdot\|_F$ returns the summation of the absolute squares of the input matrix elements, and $\mathbf{X}_{(1)} \in \mathbb{C}^{D\times LN}$ denotes the matricization of the tensor $\mathcal{X} \in \mathbb{C}^{D\times L\times N}$ with respect to the columns. The most popular algorithm for calculating the tensor subspaces is the TUCKER-Alternating Least Squares (ALS); the main idea behind this method is to solve for one factor matrix at a time by fixing the rest. In that way, each subproblem is reduced to a linear least-squares problem solved by singular value decomposition. A detailed presentation of TUCKER, and the respective solvers is offered in [22] and [23]–[25].

D. Iteratively Refined L_1-norm Tensor Subspaces

L_2-norm matrix and tensor decompositions are susceptible to corrupted, highly deviating, irregular measurements in the received signal record, such as impulsive noise. A promising approach to PCA and TUCKER with increased robustness to outliers is L_1-norm based tensor decompositions [26], [27]. The tensor subspaces are continuously refined by of calculating the conformity of each received signal element with respect to the rest. The calculated tensor subspaces indicate unprecedented subspace estimation performance and resistance to intermittent disturbances.

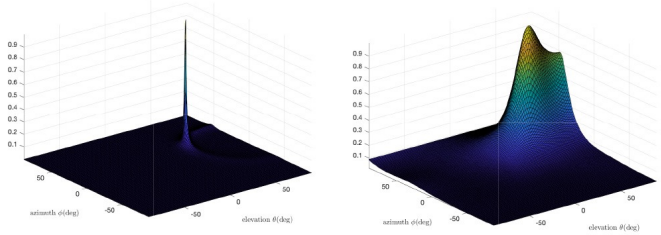

Fig. 5. Azimuth and elevation pseudo-spectra for L_1-norm [26] (Left) and L_2-norm tensor decompositions [22] (Right) of beacon 1.

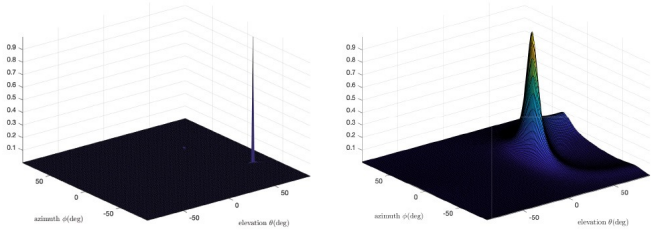

Fig. 6. Azimuth and elevation pseudo-spectra for L_1-norm [26] (Left) and L_2-norm [22] tensor decompositions (Right) of beacon 2.

IV. Performance Evaluation

We evaluate the performance of the proposed DoA estimation scheme in terms of root-mean-squared error (RMSE). The performance of the DoA estimation scheme is compared to state-of-the-art matrix and tensor L_2-norm based DoA estimation techniques. We consider two beacons transmitting time-domain coded waveforms to a triangular hydrophone array receiver. Simulations are carried out using time-varying channel realizations, generated by an UW-A channel simulator [19] that follows the statistical model in [28]. As depicted in Fig. 1, we consider two beacons deployed in a 20 m deep UW-A channel. The beacons are fixed at 9 m and 12 m, above the seabed, and positioned 500 m and 300 m away from the hydrophone array receiver. The receiver array is fixed at 5 m above the seabed. From this geometry, propagation paths and delays are calculated for each beacon. Channel variations that account for effects such as surface scattering are introduced to the simulation studies, while ambient noise is generated according to (8).

In our simulations, the coherence time of small-scale channel variations is set to 1 s. The channel gains for the simulated UW-A channel are depicted in Fig. 2 and Fig. 3 as a function of induced time delay. We consider frame transmissions of binary phase-shift keying (BPSK) symbols. The beacons utilize Hadamard codes of length $L = 4$ for their transmissions at frequency $f_c = 5$ KHz using bandwidth $B = 1$ KHz and roll-off factor $\alpha = 0.6$.

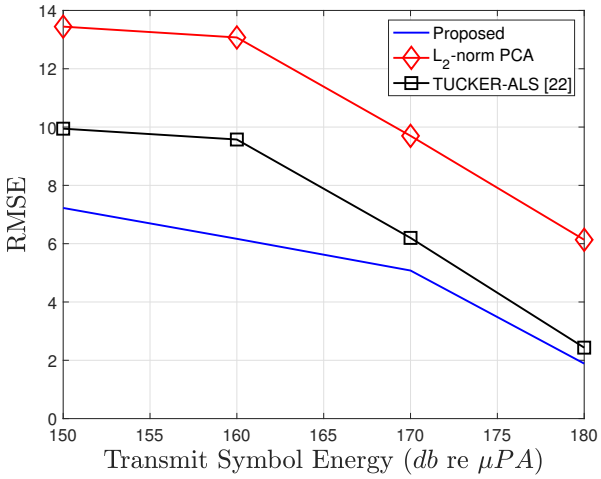

Fig. 7. Root-mean-squared-error (RMSE) of the proposed DoA estimation method after beacon identification (for the first beacon node, 300 m) vs. state-of-the-art tensor and matrix processing techniques.

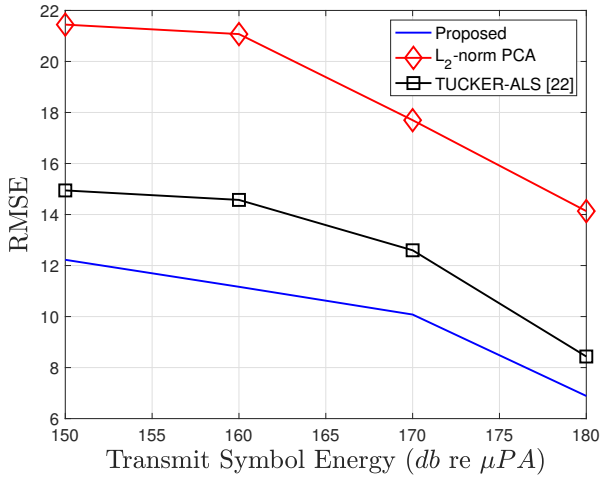

Fig. 8. Root-mean-squared-error (RMSE) of DoA estimation after beacon identification for beacon 2.

Fig. 4 depicts the pseudo-spectra of the elevation and azimuth angles-of-arrival calculated according to (13) prior to utilizing each beacon's code to identify the beacon of interest. It is clear that L_1-norm tensor analysis offers superior DoA estimation performance compared to its L_2-norm counterpart. Fig. 5 and Fig 6 depict the pseudo-spectra corresponding to the elevation and azimuth angles calculated according to (17) after utilizing the estimated beacon code to identify the triplet $(\phi, \theta, \mathbf{d})$. It is clear that the proposed iteratively-refined L_1-norm tensor decomposition method [26] produces a disturbance-free, uncorrupted spectrum (Fig. 5-Left), in contrast to the TUCKER-ALS [22] spectrum which is contaminated by the underwater channel variations and disturbances (Fig. 5-Right).

Fig. 7 depicts the RMSE defined as

$$RMSE_k = \sqrt{\frac{1}{N}\sum_{n=1}^{N}\left(\phi_k - \hat{\phi}_n\right)^2 + \left(\theta_k - \hat{\theta}_n\right)^2}, k = 1, \ldots, K \tag{19}$$

for the proposed DoA estimator for the first beacon node (300 m) as a function of the transmitted symbol energy E_k in dB re μPa. The RMSE is calculated over $N = 5000$ independent trials. The true azimuth and elevation angles of arrival for the two beacons are assumed to be $(\phi_1 = 30^\circ, \theta_1 = 40^\circ)$, and $(\phi_2 = -30^\circ, \theta_2 = 60^\circ)$. The transmitted symbol energy was fixed to be equal for both beacon nodes. The L_1-norm tensor DoA technique is compared to L_2-norm PCA space-time processing, and L_2-norm TUCKER-ALS tensor processing [22] methods. As shown, the proposed DoA estimation method offers significantly better RMSE performance. Similar RMSE performance can be observed for the second beacon node (500 m) in Fig. 8.

V. Conclusions

We present and evaluate for the first time the performance of a beacon-assisted underwater localization system that can be utilized for 3D self-localization of AUVs. Robust DoA-guided localization of the AUVs is achieved by iteratively refined L_1-norm space-time tensor subspaces. The proposed localization system leverages the tensor structure of space-time coded reference beacon signals at the input of a triangular hydrophone array (that will be mounted on the AUV) to jointly estimate the angles-of-arrival of the beacons, as well as, identify the codes corresponding to each beacon. Simulation studies verify the superiority of the proposed localization technique compared to state-of-the-art L_2-norm based tensor and matrix DoA estimation methods.

References

[1] E. An, M. R. Dhanak, L. K. Shay, S. Smith, and J. Van Leer, "Coastal oceanography using a small auv," *Journal of Atmospheric and Oceanic Technology*, vol. 18, no. 2, pp. 215–234, 2001.

[2] K. DeMarco, M. E. West, and T. R. Collins, "An implementation of ros on the yellowfin autonomous underwater vehicle (auv)," in *OCEANS'11 MTS/IEEE KONA*, Sep. 2011, pp. 1–7.

[3] V. L. Lucieer and A. L. Forrest, *Emerging Mapping Techniques for Autonomous Underwater Vehicles (AUVs)*. Springer International Publishing, 2016, pp. 53–67.

[4] A. Diercks, M. Woolsey, R. Jarnagin, V. L. Asper, C. Dike, M. D'Emidio, S. Tidwell, and A. Conti, "Site reconnaissance surveys for oil spill research using deep-sea auvs," in *2013 OCEANS*, Sep. 2013, pp. 1–5.

[5] E. Demirors, G. Sklivanitis, T. Melodia, S. N. Batalama, and D. A. Pados, "Software-defined underwater acoustic networks: toward a high-rate real-time reconfigurable modem," *IEEE Communications Magazine*, vol. 53, no. 11, pp. 64–71, Nov. 2015.

[6] G. T. Donovan, "Position error correction for an autonomous underwater vehicle inertial navigation system (ins) using a particle filter," *IEEE Journal of Oceanic Engineering*, vol. 37, no. 3, pp. 431–445, Jul. 2012.

[7] D. Ribas, P. Ridao, J. D. Tards, and J. Neira, "Underwater slam in man-made structured environments," *Journal of Field Robotics*, vol. 25, pp. 898–921, 2008. [Online]. Available: https://onlinelibrary.wiley.com/doi/abs/10.1002/rob.20249

[8] D. Thomson and S. Dosso, "Auv localization in an underwater acoustic positioning system," in *2013 MTS/IEEE OCEANS - Bergen*, June 2013.

[9] R. Kaune, J. Horst, and W. Koch, "Accuracy analysis for tdoa localization in sensor networks," in *Proc. Int. Conf. on Inf. Fus.*, Jul. 2011.

[10] D. Moreno-Salinas, A. Pascoal, and J. Aranda, "Optimal sensor placement for acoustic underwater target positioning with range-only measurements," *IEEE J. Oceanic Eng.*, vol. 41, no. 3, pp. 620–643, Jul. 2016.

[11] G. Vallicrosa, P. Ridao, D. Ribas, and A. Palomer, "Active range-only beacon localization for auv homing," in *2014 IEEE/RSJ International Conference on Intelligent Robots and Systems*, Sep. 2014.

[12] I. Masmitja, S. Gomariz, J. Del-Rio, B. Kieft, T. OReilly, P. J. Bouvet, and J. Aguzzi, "Optimal path shape for range-only underwater target localization using a wave glider," *The International Journal of Robotics Research*, vol. 37, no. 12, pp. 1447–1462, 2018.

[13] S. Barkby, S. Williams, O. Pizarro, and M. Jakuba, "An efficient approach to bathymetric slam," in *2009 IEEE/RSJ International Conference on Intelligent Robots and Systems*, Oct 2009, pp. 219–224.

[14] Luyue Huang, Bo He, and Tao Zhang, "An autonomous navigation algorithm for underwater vehicles based on inertial measurement units and sonar," in *2010 2nd International Asia Conference on Informatics in Control, Automation and Robotics (CAR 2010)*, vol. 1, March 2010.

[15] F. Demim, A. Nemra, H. Abdelkadri, A. Bazoula, K. Louadj, and M. Hamerlain, "Slam problem for autonomous underwater vehicle using svsf filter," in *2018 25th International Conference on Systems, Signals and Image Processing (IWSSIP)*, June 2018, pp. 1–5.

[16] N. Tsagkarakis, P. P. Markopoulos, and D. A. Pados, "Direction finding by complex l1-principal-component analysis," in *2015 IEEE 16th International Workshop on Signal Processing Advances in Wireless Communications (SPAWC)*, June 2015, pp. 475–479.

[17] X. Zhong, A. B. Premkumar, and W. Wang, "Direction of arrival tracking of an underwater acoustic source using particle filtering: Real data experiments," in *IEEE 2013 Tencon - Spring*, April 2013.

[18] N. Tsagkarakis, P. P. Markopoulos, G. Sklivanitis, and D. A. Pados, "L1-norm principal-component analysis of complex data," *IEEE Transactions on Signal Processing*, vol. 66, no. 12, pp. 3256–3267, June 2018.

[19] P. Qarabaqi and M. Stojanovic, "Acoustic channel modeling and simulation," http://millitsa.coe.neu.edu/?q=projects.

[20] R. J. Urick, *Principles of Underwater Sound*, 3rd ed. McGraw-Hill, 1983.

[21] M. Stojanovic, "Acoustic communication," in *Springer Handbook of Ocean Engineering*. Springer, 2016, ch. 15, pp. 359–386.

[22] N. D. Sidiropoulos, L. De Lathauwer, X. Fu, K. Huang, E. E. Papalexakis, and C. Faloutsos, "Tensor decomposition for signal processing and machine learning," *IEEE Transactions on Signal Processing*, vol. 65, no. 13, pp. 3551–3582, July 2017.

[23] T. Kolda and B. Bader, "Tensor decompositions and applications," *SIAM Review*, vol. 51, no. 3, pp. 455–500, 2009.

[24] J. Sun, D. Tao, S. Papadimitriou, P. S. Yu, and C. Faloutsos, "Incremental tensor analysis: Theory and applications," *ACM Trans. Knowl. Discov. Data*, vol. 2, no. 3, pp. 1–37, Oct. 2008.

[25] X. Li, M. K. Ng, G. Cong, Y. Ye, and Q. Wu, "Mr-ntd: Manifold regularization nonnegative tucker decomposition for tensor data dimension reduction and representation," *IEEE Transactions on Neural Networks and Learning Systems*, vol. 28, no. 8, pp. 1787–1800, Aug 2017.

[26] K. Tountas, D. A. Pados, and M. J. Medley, "Conformity evaluation and l_1-norm principal-component analysis of tensor data," *Proc. SPIE Big Data: Learning, Analytics, and Applications*, May 2019.

[27] P. P. Markopoulos, D. G. Chachlakis, and E. E. Papalexakis, "The exact solution to rank-1 l1-norm tucker2 decomposition," *IEEE Signal Processing Letters*, vol. 25, no. 4, pp. 511–515, April 2018.

[28] P. Qarabaqi and M. Stojanovic, "Statistical characterization and computationally efficient modeling of a class of underwater acoustic communication channels," *IEEE Journal of Oceanic Engineering*, vol. 38, no. 4, pp. 701–717, Oct 2013.